*Journal of Applied Chemistry* **JAC**
http://chemistry.journals.semnan.ac.ir

# Investigation the performance of $KO_2$-fiberglass nanocomposite in $O_2$ supply and $CO_2$ removal in closed human respiratory environments

**Rahil Shokouhian, Manoochehr Fathollahi*, Seyed Ghorban Hosseini, Seyed Hadi Motamedalshariaty**
*Department of Chemistry, Malek Ashtar University of Technology*

*Article history:*
*Received:27/ Jan /2020*
*Received in revised form: 18/Feb/2020*
*Accepted: 23/Feb/2020*

**Abstract**

Potassium superoxide-fiberglass nanocomposite is chemical oxygen source and carbon dioxide removal that can be used in human air revitalization systems. The potassium superoxide ($KO_2$) nanoparticles as a part of the nanocomposite were synthesized by the electrohydrodynamic (EHD) method and coated on the fiberglass support as the second part of the nanocomposite. To investigate the morphology of synthesized nanocomposite ($KO_2$-fiberglass), field emission scanning electron microscopy (FESEM) was employed. The results showed that the $KO_2$-fiberglass nanocomposite obtained by EHD has a uniform structure in the nanometer dimension. To simulate oxygen generation and carbon dioxide removal of the nanocomposite, a human-like lung simulated (HLLS) set-up was designed and made. Experimental studies in the HLLS set-up were performed under different humidity and the effect of humidity was investigated on the changes of oxygen and carbon dioxide concentration. Consequently, studying data showed that $KO_2$-fiberglass nanocomposite has suitable performance as air revitalization because increases oxygen amounts up to 29.4 percentage. Also, carbon dioxide amount is decreased to half, which is twice faster than of commercial $KO_2$ samples (in 60min). Moreover, the higher amount of humidity (85%) and temperature (45ºC), as a catalyst, causes an increased rate of $CO_2$ removal and $O_2$ generation. . Besides, the reaction rate constants were estimated by a kinetic model of nanocomposite of $KO_2$ and the activation energy of the process was calculated. The kinetic model of nanocomposite oxygen release proved that the reaction model is D4 and the amount of Ea is $12kJ.mol^{-1}$.

**Keywords**: Respiratory air revitalization, Potassium superoxide/fiberglass nanocomposite, Oxygen generation, Carbon dioxide removal.

*. **Corresponding author:** Assistant Professor of Physical Chemistry, Malek Ashtar University of Technology, Department of Chemistry, Tehran, Iran. mfathollahi@alumni.ut.ac.ir

## 1. Introduction

Air revitalization is based on chemicals such as superoxides, especially potassium and sodium superoxide [1–3]. They have chemical oxygen bound released by exposure to air moisture. Also, they are employed as oxidants and sources of oxygen. Typically, two methods were employed for supplying oxygen; (1) physical, and (2) chemical methods [4, 5]. The physical method uses compressed oxygen or air to generate oxygen [4], and the chemical one applies chemical oxygen compounds such as alkali metal chlorates/perchlorates and alkali metal peroxides/superoxides to generate oxygen [6]. Among these methods, the chemical ones provide high yield oxygen [7]. Each of the chemical oxygen sources has some advantages and disadvantages which is determined by reaction condition. For example, oxygen supply is provided by alkali metal chlorates/perchlorates rapidly, while they produce high amounts of heat immediately [8, 9]. In another example, alkali metal peroxides/superoxides generate oxygen by adsorption of carbon dioxide and other harmful gases; however, they are susceptible to environmental conditions, and controlling them is difficult [10]. The respiratory system (also respiratory apparatus, ventilatory system) is a biological system consisting of specific organs and structures used for gas exchange in animals and plants. In human exhaled air, the concentration of oxygen and carbon dioxide changes. The amount of oxygen varies between 21% - 19%, and carbon dioxide 5.6 - 3.6% (as shown in table 1 and 2 respectively) [11].

The oxygen supply methods commonly used in spaces with failure of $O_2$, contains high-pressure oxygen storage, liquid oxygen storage at low temperature, and chemical oxygen [12].

**Table 1.** effect of oxygen efficiency

| Present oxygen in the air | Effect |
|---|---|
| 17 | Faster, deep breathing |
| 15 | Dizziness, buzzing in ears, rapid heartbeat |
| 13 | May loss consciousness |
| 9 | Fainting, unconsciousness |
| 7 | Life endangered |
| 6 | Convulsive movement, death |

**Table 2.** effect of carbon dioxide concentration

| $CO_2$ concentration | time | effect |
|---|---|---|
| 17-30 | Within 1 min | Loss of controlled and purposeful activity, unconsciousness, convulsions, coma, death |
| 10-15 | 1 min to several min | Dizziness, drowsiness, severe muscle twitching, unconsciousness |
| 7-10 | Few minutes | Unconsciousness, near unconsciousness |
| | 1.5 minutes to 1 hour | Headache, increased heart rate, shortness of breath, dizziness, sweating, rapid breathing |
| 6 | 1-2 min | Hearing and visual disturbances |
| | ≥ 16 min | Headache, dyspnea |
| | Several hours | tremors |
| 4-5 | Within a few minutes | Headache, Dizziness, increased blood pressure, uncomfortable dyspnea |
| 3 | 1 hour | Mild headache, sweating, dyspnea at rest |
| 2 | Several hours | Headache, dyspnea upon mild exertion |

Several kinds of chemical oxygen sources include superoxides, oxygen candles, percarbonates, and liquid hydrogen peroxide [12]. Such oxygen source with characteristics of small volume, lightweight, easy to carry, simple to use, and high oxygen production, is needed for keeping ordnance, rescuing injured, using in spacecraft, submarines and etc. Therefore, chemical oxygen has been paid more attention from scientists [12]. Among all chemical oxygen sources, potassium superoxide, a heat and moisture-sensitive substance, is mostly used. The reaction between $KO_2$ and $H_2O$ occurred at ambient, and higher temperatures cause hydroxide and hydrated hydroxide during reaction with the evolution of $O_2$ gases. It is used as a two-function material for air revitalization is made in two forms; tablet and plate [12, 13]. They have advantages like small size, large oxygen storage per unit volume, absorbing carbon dioxide while providing oxygen, without consuming power and etc., make them be applied as the main choice of the chemical oxygen sources [12]. Small tablet-like potassium superoxide (STLP) is commonly used as a self-rescuer in poor places of $O_2$ [15]. Also, the larger plate-like potassium superoxide (PLPS) is used in submarines [16] and spacecraft [17]. One of the best choices of chemical oxygen sources is superoxide. Superoxide reacts with carbon dioxide and then oxygen is generated in the presence of water vapor. Consequently, granular and laminar potassium superoxide products have been developed. Recently, researchers attempted to combine potassium superoxide with a silicone polymer matrix or glass fiber matrix to improve the reaction stability [3, 17]. In this study, the air revitalization performance of synthesized $KO_2$-fiberglass nanocomposite as an air revitalization (AR) compound was synthesized by the electrohydrodynamic (EHD) method and investigated under static reaction conditions in a sealed reaction chamber. By analyzing the evolution of oxygen and carbon dioxide inside the chamber under experimental conditions (initial reaction temperature, humidity, and carbon dioxide concentration), the application of nanocomposite plate of AR was investigated and compared with other reported samples.

## 2. Experimental procedure

### 2. 1 Materials and method

All chemical reagents were analytical grade and used as received without further purification. Deionized and doubly distilled water, Aqueous hydrogen peroxide solution 50% (V/V) and potassium hydroxide 90% (W/W), cobalt nitrate, and magnesium sulfate were all purchased from Merck (Tehran, Iran). Commercial fiberglass, as high-porosity polymeric support, was purchased from Qinhuangdao Dinuo technology Development carbon dioxide, oxygen, temperature, and humidity sensors were used to measure carbon dioxide and oxygen levels, temperature, and humidity during performance testing of samples. Table 3 provides a summary of the technical specifications of the used sensors.

### 2. 2 Experimental set-up

The performance of respiratory air-revitalization compounds in a laboratory environment simulating human respiration is investigated using the required sensors. The $KO_2$-fiberglass nanocomposite was employed in a sealed chamber to investigate air revitalization performance.

**Table 3.** Technical specifications of sensors

| **Sensor type** | Model | Range | Precision | Accuracy |
|---|---|---|---|---|
| **Carbon dioxide** | Testo 535 (Germany) | 0 to 9999 ppm | 1 ppm | ± (3% + 75 ppm) from 0 to 5000 ppm<br>± (5% + 150 ppm) from 5000 to 9999 ppm |
| **Oxygen (%)** | Step System (Germany) | 0 to 100% | 0.1% | ±0.4 mg/l of dissolved oxygen in the air |
| **Humidity Ratio (%)** | LUTRON YK-90HT (Taiwan) | 10 % to 95 % | 0.1 % | ≧70% RH: ± (3% reading + 1% RH).<br>< 70% RH: ± 3% RH |
| **Temperature (°C)** | LUTRON YK-90HT (Taiwan) | 0 to 50 °C, 32 to 122 °f | 0.1 Degree | °C -0.8 °C, °F - 1.5. °F |

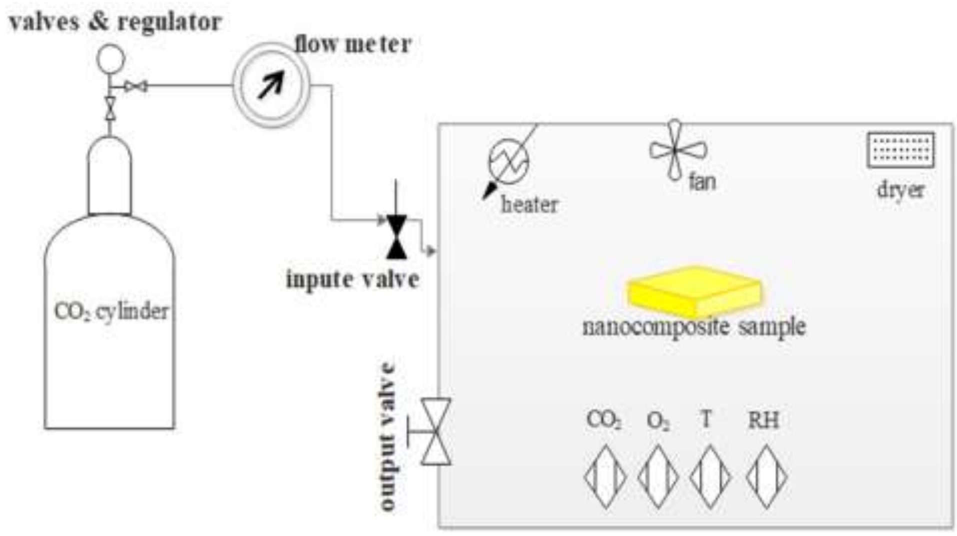


**Fig. 1**. Schematic illustration of the functional test device

To this purpose, a Plexiglass box with 60×60×60 cm in length, width, height was selected. The schematic of this set-up is shown in Fig 1. This device contains sensors of carbon dioxide, oxygen, temperature, and humidity measurement and also, heater and humidifier. Sealing polymers made of EPDM Rubber to seal the device and polyurethane adhesives to insulate the device.

Adjusting the temperature, humidity, and carbon dioxide level was performed by a carbon dioxide gas cylinder with 99.99% concentration, humidifier, and a 100 (w) lamp as a heater.

**2.3 Experimental method:**

The $KO_2$-fiberglass nanocomposite was synthesized in previous [19]. Typically, the solution of hydrogen peroxide was prepared at first. Then, a particular piece of polymeric support was impregnated in the $H_2O_2$ solution and was exposed to a high voltage electric field finally, which caused $KO_2$ to be synthesized on support. Then, the function of synthesized nanocomposite was investigated by simulated human respiratory set-up. To this purpose, a piece of nanocomposite sample in 5mm length, 5mm width, 2mm thickness, and 3g of weight containing 29.5% active oxygen content was used. This nanocomposite was put in the sealed and isolated chamber(device).

In this experiment, parameters such as temperature, humidity, and carbon dioxide concentration were adjusted on 23, 29, 35, and 45 °C, and 17, 25, 5, and 85%, and 9,000 ppm, respectively. The reaction begins immediately after the nanocomposite is exposed to moisture. At the beginning of the test, changes in the experiment environment, the concentration of carbon dioxide, and oxygen were recorded at times of 5,10,15,20, 35, and 60 min.

**2.4 Active oxygen content and carbon dioxide absorption rate measurement**

To determine the active oxygen content of the $KO_2$-fiberglass nanocomposite at the beginning of the test, a piece of weighted synthesized $KO_2$-fiberglass nanocomposite was put in a beaker. Then, 10 ml of the aqueous solution of cobalt nitrate 5% (W/V) was added to the beaker contains nanocomposite. After minutes, oxygen bubbles were generated and the total weight of the sample was reduced. The active oxygen content was calculated by the equation (1):

$$Oxygen\ (\%) = \frac{w_i - w_f}{w_i} \cdot 100 \quad (1)$$

$W_i$ is the initial and $W_f$ is the final weight of the synthesized nanocomposite sample.

To calculate the $CO_2$ absorption rate of the nanocomposite, equation (2) was used:

$$WCO2 = \frac{C_{ico2} - C_{fco2}}{\Delta t} \quad (2)$$

$WCO_2$ (mg/L.min) is the rate of carbon dioxide absorption by nanocomposite based on potassium superoxide. $C_{iCO2}$ is the initial concentration of carbon dioxide at the start of the air recovery process, $C_{fCO2}$ is the final concentration of carbon dioxide at the end of the process, and Δt is the time of test (min) [20].

**2.5 Method of calculating kinetic parameters**

The degree conversion of reaction (α) parameter can be used to calculate the kinetic parameters. The value of α varies between 0 and 1 and measures the rate of reaction progress. On the other hand, the constant relationship between rate constant and temperature is expressed through the Arrhenius equation [21]. Where A is the pre-exponential (frequency) factor, Ea is the activation energy, T is the absolute temperature and R is the gas constant.

**Table 4.** Rate expressions for different reaction models [22]

| Reaction model | | Integral model $g(\alpha) = k\,t$ |
|---|---|---|
| Nucleation models | P2 | $\alpha^{1/2}$ |
| | P3 | $\alpha^{1/3}$ |
| | P4 | $\alpha^{1/4}$ |
| | A2 | $[-\ln(1-\alpha)]^{1/2}$ |
| | A3 | $[-\ln(1-\alpha)]^{1/3}$ |
| | A4 | $[-\ln(1-\alpha)]^{1/4}$ |
| Geometrical contraction models | R2 | $[1-(1-\alpha)^{1/2}]$ |
| | R3 | $[1-(1-\alpha)^{1/3}]$ |
| Diffusion models | D1 | $\alpha^2$ |
| | D2 | $[(1-\alpha)\ln(1-\alpha)] + \alpha$ |
| | D3 | $[1-(1-\alpha)^{1/3}]^2$ |
| | D4 | $1-(2\alpha/3) - (1-\alpha)^{2/3}$ |
| Reaction-order models | F0/R1 | $\alpha$ |
| | F1 | $-\ln(1-\alpha)$ |
| | F2 | $(1-\alpha)^{-1}-1$ |
| | F3 | $0.5[(1-\alpha)^{-2}-1]$ |

$$k = Ae^{\frac{-Ea}{RT}} \quad (3)$$

The integral model of the reaction is as follows. The different reaction models that are more used in this category of reactions are shown in Table 4 [23].

$$g(\alpha) = kt \quad (4)$$

**3. Results and discussion**

**3.1 Reaction process of potassium superoxide**

Potassium superoxide does not react with carbon dioxide in dry air because the heat of this reaction has been estimated to be 43.1 kcal [24].

$$KO_2+CO_2 \rightarrow K_2CO_3+1.5O_2 \quad (5)$$

Therefore, achieve the high heat of the reaction, is almost impossible. In the reaction of $KO_2$ with moisture containing carbon dioxide at 10°C or less, the $K_2C_2O_6$ is formed and only the superoxide's oxygen is released. At 50°C or above, all active oxygen is released with the formation of potassium carbonate and bicarbonate [25].

The reaction of moisture-containing $CO_2$ with $KO_2$ can be caused to the formation of $KHCO_3$ at 60°C and below. Under these conditions, the ratio of absorbed $CO_2$ to released oxygen is more than 0.67 [26].

Under experimental conditions, the chemical reaction equations of nanocomposite plates are as follows (see Eqs (6)– (8)):

At first, the nanocomposite plates with bright yellow-color react with ambient $CO_2$ directly, then potash formed and oxygen released (Eq (4)).

$$4KO_2+2CO_2 \rightarrow 2K_2CO_3+3O_2 \quad (6)$$

In this section, adsorbing of ambient water vapor onto its surface, forming orange-colored plate hydrate, which subsequently reacts with further water vapor to form white potassium hydroxide and then oxygen release (Eq (5)).

$$4KO_2+2H_2O \rightarrow 4KOH+3O_2 \quad (7)$$

Now, Potassium hydroxide continues to react with $CO_2$ to produce potash and water. here, water plays a role as a sort of autocatalyst in the oxygen generation of plates (Eq (6)). Therefore, the reaction of $KO_2$ with $CO_2$ and the generation of $O_2$ is affected by the amount of humidity.

$$2KOH+CO_2 \rightarrow K_2CO_3+H_2O \quad (8)$$

**3.2 $CO_2$ Conversion to Oxygen in the Presence of $KO_2$-fiberglass Nanocomposite**

As can be seen in Table 5(a-d) and Fig. 2(a, b), over time, with the intense absorption of $CO_2$ in the environment by the $KO_2$-fiberglass nanocomposite, under different humidity, a sharp decrease in ambient $CO_2$ and an increase in the amount of $O_2$ occur. Even the data in Table

6(a-c) and Fig. 3(a,b) show that over time, the absorption of $CO_2$ and generation of $O_2$ increased by increasing temperature.

As shown in Fig. 2b and 3b, it obvious that there is a decrease in the concentration of existing $CO_2$ during the experiment from start to the endpoint, and the slope of the curve decreases by the time till the stabilization of the reaction ends. It is because of the $KO_2$-fiberglass nanocomposite reaction with existing $CO_2$, which lows the $CO_2$ concentration. While the reaction continued, the amount of $KO_2$ and the other products refuse the reaction to be continued and decreasing the reaction rate [27]. The synthesized $KO_2$ not only reacts with $CO_2$ but also hydrated. So, this subject causes the concentration of $CO_2$ decreased by adsorption of KOH.

Table 5 and Fig. 5(a, b) show the effect of moisture on the performance of the $KO_2$-fiberglass nanocomposite. It is obvious that with increasing humidity, the $KO_2$-fiberglass nanocomposite produces more $O_2$ and absorbs more $CO_2$ quickly. The reason for this phenomenon is that $KO_2$ is hygroscopic and reacts strongly with water and absorbs carbon dioxide so produces oxygen and potassium hydroxide at a higher rate. As Table 5 shows, the amount of produced oxygen increases from 1.1 to 1.5 times with increasing humidity at a constant time.

**Table 5.** Variation of carbon dioxide concentration and amount of oxygen in the $KO_2$-fiberglass nanocomposite medium over time with9000ppm of initial $CO_2$ concentration and 19.2% of active $O_2$ under four different humidity conditions a)17%, b)25%, c)50% and d)85%

| (a) | | | (b) | | |
|---|---|---|---|---|---|
| **T(min)** | **$CO_2$%** | **$O_2$%** | **T(min)** | **$CO_2$%** | **$O_2$%** |
| 5 | 8674 | 19.3 | 5 | 8143 | 19.3 |
| 10 | 7957 | 20 | 10 | 6920 | 20 |
| 15 | 7086 | 20 | 15 | 6266 | 20.4 |
| 20 | 6731 | 20.4 | 20 | 5963 | 21.6 |
| 35 | 6258 | 20.6 | 35 | 5293 | 22.3 |
| 60 | 5763 | 20.8 | 60 | 4884 | 22.7 |

| (c) | | | (d) | | |
|---|---|---|---|---|---|
| **T(min)** | **$CO_2$%** | **$O_2$%** | **T(min)** | **$CO_2$%** | **$O_2$%** |
| 5 | 7851 | 20.4 | 5 | 7408 | 20.9 |
| 10 | 6548 | 21.6 | 10 | 6326 | 22 |
| 15 | 5832 | 22.8 | 15 | 5481 | 24.7 |
| 20 | 5127 | 24 | 20 | 4784 | 26.6 |
| 35 | 4641 | 25.7 | 35 | 4108 | 28.1 |
| 60 | 4002 | 26.5 | 60 | 3561 | 29.4 |

**Table 6.** Variation of carbon dioxide concentration and amount of oxygen in the $KO_2$-fiberglass nanocomposite medium over time with9000ppm of initial $CO_2$ concentration and 19.2% of active $O_2$ under four different temperature conditions a)23, b)29, c)35, and d)45ºC

| (a) | | | (b) | | |
|---|---|---|---|---|---|
| **T(min)** | **$CO_2$%** | **$O_2$%** | **T(min)** | **$CO_2$%** | **$O_2$%** |
| 5 | 8318 | 19.3 | 5 | 7513 | 19.6 |
| 10 | 7879 | 19.7 | 10 | 6920 | 20.8 |
| 15 | 7521 | 19.8 | 15 | 6266 | 21.6 |
| 20 | 7312 | 20.2 | 20 | 5963 | 22.8 |
| 35 | 6794 | 20.7 | 35 | 5293 | 23.7 |
| 60 | 6001 | 20.9 | 60 | 4884 | 24.2 |

| (c) | | | (d) | | |
|---|---|---|---|---|---|
| **T(min)** | **$CO_2$%** | **$O_2$%** | **T(min)** | **$CO_2$%** | **$O_2$%** |
| 5 | 8084 | 21.4 | 5 | 7724 | 23.6 |
| 10 | 7003 | 22.9 | 10 | 6586 | 25.6 |
| 15 | 6168 | 24.7 | 15 | 5721 | 26.4 |
| 20 | 5278 | 25.8 | 20 | 4894 | 27.3 |
| 35 | 4512 | 26.9 | 35 | 4352 | 28.4 |
| 60 | 4095 | 27.4 | 60 | 3002 | 28.7 |

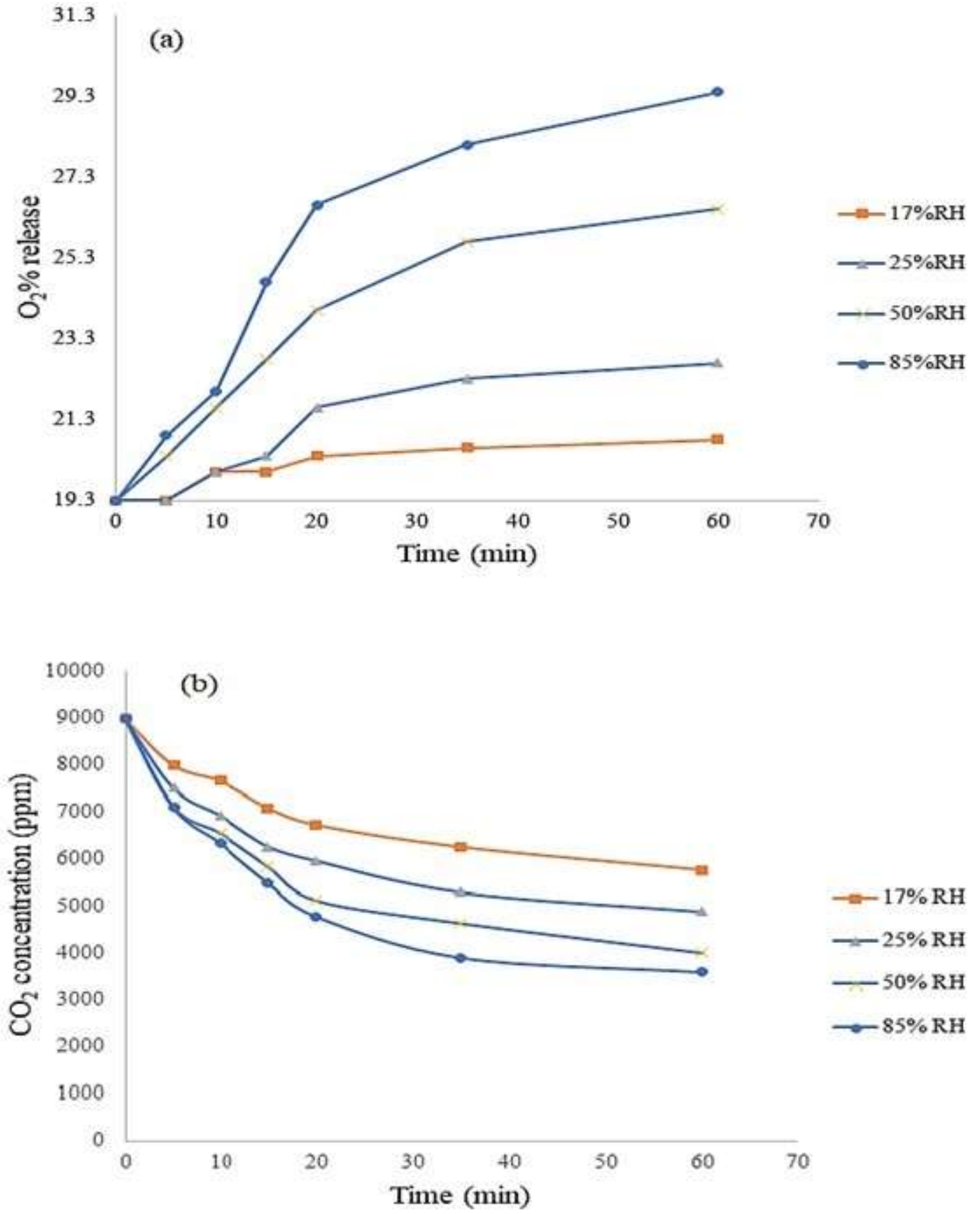


**Fig. 2.** The process of (a) oxygen generation and (b) absorption of carbon dioxide during 60 minutes for $KO_2$-fiberglass nanocomposite under different humidity

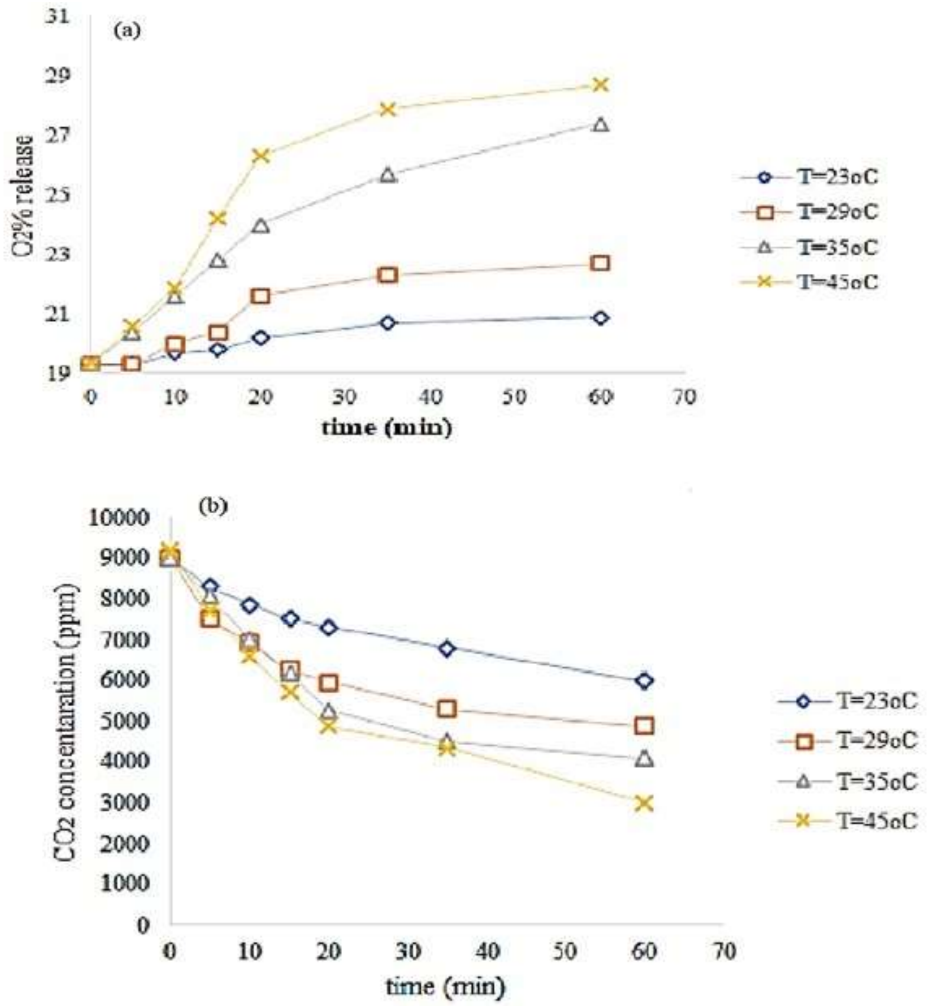


**Fig. 3.** The process of (a) oxygen generation and (b) absorption of carbon dioxide during 60 minutes for $KO_2$-fiberglass nanocomposite at different temperature

**Table 7.** Basic conditions and experimental data of nanocomposite plates under different humidity and 29ºC temperature

| **operating condition** | humidity RH% | initial $O_2$% | final $O_2$% | initial $CO_2$% | final $CO_2$% | time (min) |
|---|---|---|---|---|---|---|
| **1** | 17 | 19 | 20.8 | 9006 | 5763 | 60min |
| **2** | 25 | 19 | 22.7 | 9006 | 4884 | 60min |
| **3** | 50 | 19 | 26.5 | 9006 | 4002 | 60min |
| **4** | 85 | 19 | 29.4 | 9006 | 3589 | 60min |

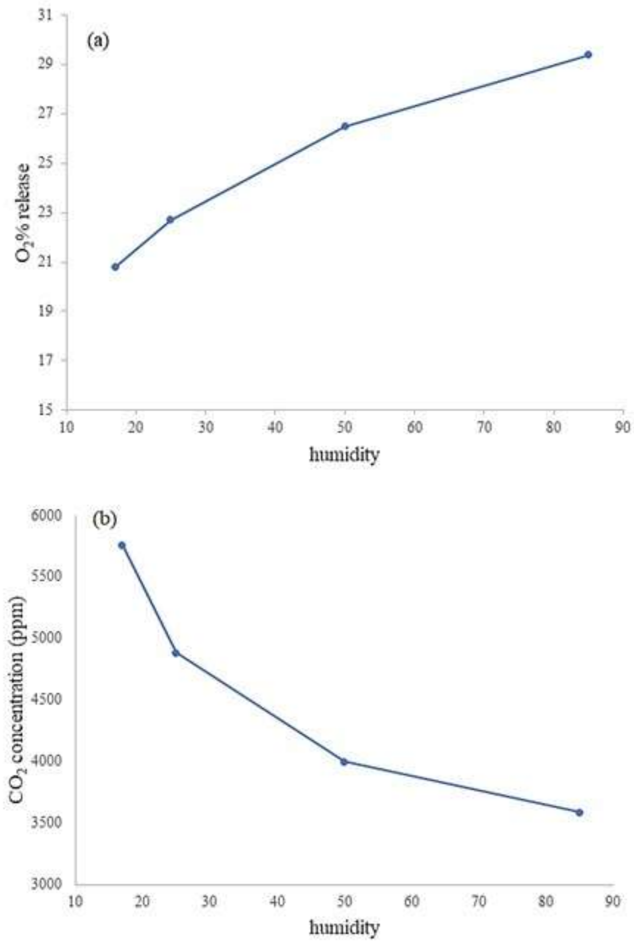


**Fig. 4.** The relationship between (a) active $O_2$% and (b) $CO_2$ concentration with humidity in functional test

**Table 8.** Basic conditions and experimental data of nanocomposite plates at different temperature and humidity of 25%

| operating condition | temperature T (ºC) | humidity RH% | initial $O_2$% | final $O_2$% | initial $CO_2$% | final $CO_2$% | time (min) |
|---|---|---|---|---|---|---|---|
| **1** | 23 | 25 | 19 | 21 | 9006 | 6001 | 60min |
| **2** | 29 | 25 | 19 | 23 | 9006 | 4884 | 60min |
| **3** | 35 | 25 | 19 | 26 | 9006 | 4095 | 60min |
| **4** | 45 | 25 | 19 | 29 | 9006 | 3002 | 60min |

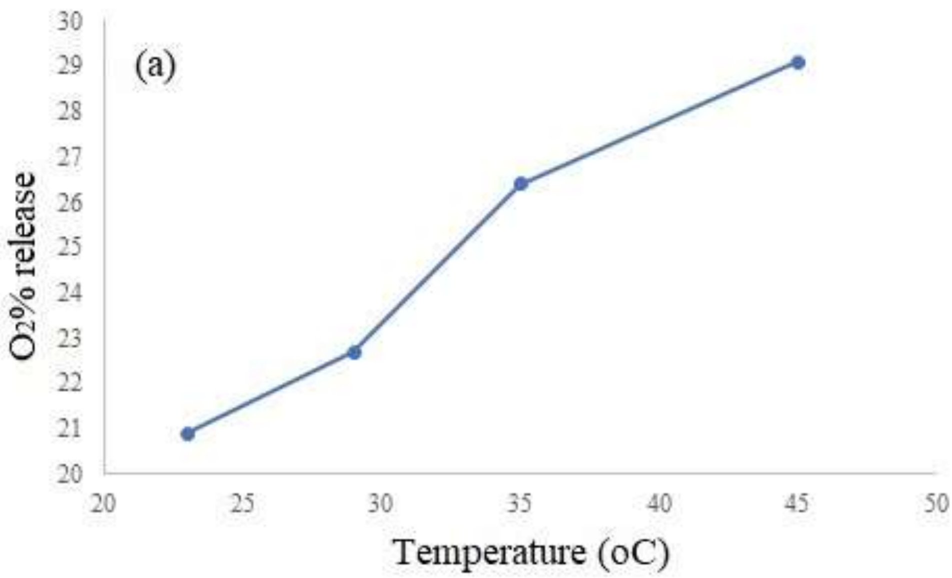


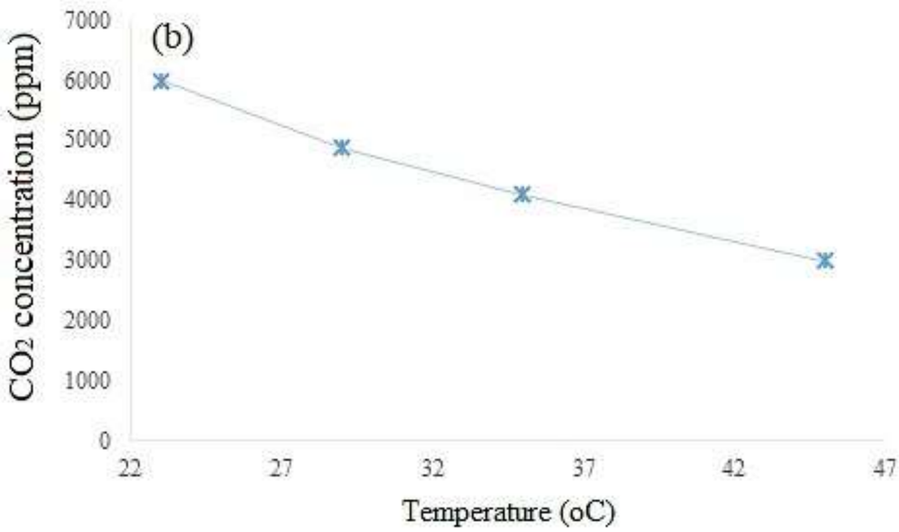


**Fig. 5.** The relationship between (a) active $O_2$% and (b) $CO_2$ concentration with temperature in functional test

Table 8 and Fig. 5(a, b) show the effect of temperature on the performance of the $KO_2$-fiberglass nanocomposite. It is obvious that with increasing temperature, the $KO_2$-fiberglass nanocomposite produces more $O_2$ and absorbs more $CO_2$ quickly. The reason for this phenomenon is that $KO_2$ is a heat-sensitive material and reacts strongly with water when the temperature increased and absorbs carbon dioxide so produces oxygen and potassium hydroxide at a higher rate.

**3.3. Comparison of the function of $KO_2$-fiberglass nanocomposite and commercial sample**

Fig. 6 shows the performance of $KO_2$-fiberglass nanocomposite in comparison with commercial products of potassium superoxide, made of $KO_2$ powder mixed with performance-modifying additives that are widely used. As shown in Fig. 4, synthesized $KO_2$-fiberglass nanocomposite under the same condition (temperature and humidity), compared to commercial samples, absorbs and produces a higher amount of carbon dioxide and oxygen, respectively. The remarkable performance of the synthesized nanocomposite compared to the commercial samples is the absorption of carbon dioxide in less time and conversion of it to oxygen.

In other words, the conversion rate of carbon dioxide to oxygen with synthesized nanocomposite plate is twice as fast as with commercial samples. Moreover, the synthesized nanocomposite plate is performance-modifying additives free, while commercial samples contain a significant percentage of additives that improve the absorption of moisture and $CO_2$.

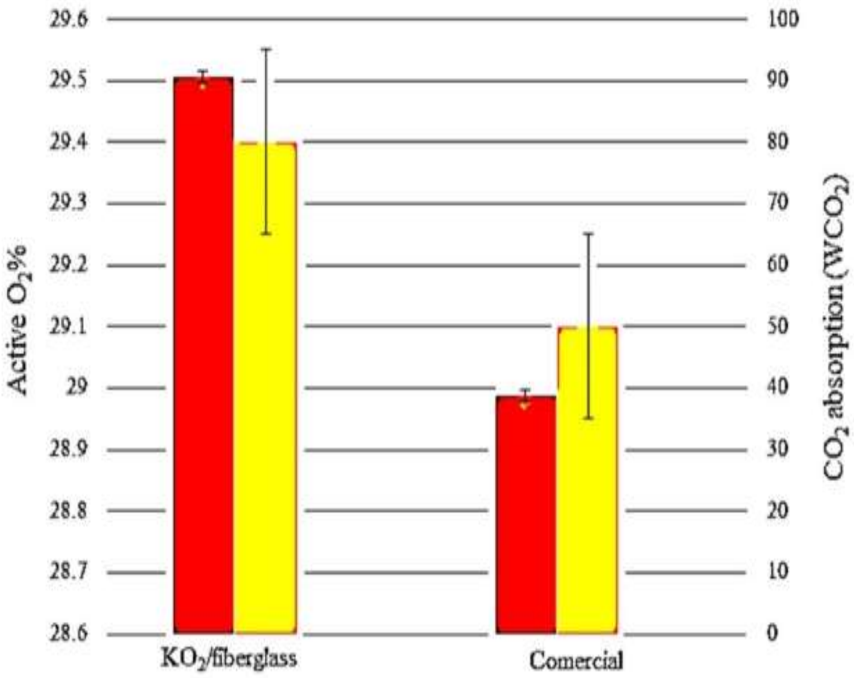


**Fig. 6.** Performance comparison chart of nanocomposite of $KO_2$-fiberglass with commercial samples

**4.3. Kinetic of the reaction:**

For each model in the Table 4 plotting g(α) versus t, a straight line can be obtained with the slope of k. The model which has the best fitting to the reaction and is describing the reaction has the highest and the lowest value for the correlation coefficient, and for the standard deviation, respectively. The fitting data is shown in Table 9. According to the basic selection criterion, the most probable kinetic function has a correlation coefficient greater than 0.98 and a standard deviation less than 0.3, the most probable kinetic function is only the equation D4 as shown in Table 9.

**Table 9.** Kinetic mechanism function and fitting result

| Model | Correlation coefficient (R) | | | | Standard deviation (SD) | | | |
|---|---|---|---|---|---|---|---|---|
| | 23ºC | 29 ºC | 35 ºC | 45 ºC | 23 ºC | 29 ºC | 35 ºC | 45 ºC |
| P2 | 0.8603 | 0.8499 | 0.7483 | 0.6519 | 0.4076 | 0.4168 | 0.3515 | 0.3497 |
| P3 | 0.7981 | 0.7944 | 0.6758 | 0.5914 | 0.4209 | 0.4267 | 0.3505 | 0.3547 |
| P4 | 0.7579 | 0.7571 | 0.6289 | 0.5573 | 0.4317 | 0.4355 | 0.3526 | 0.3586 |
| A2 | 0.9801 | 0.9821 | 0.9620 | 0.9321 | 1.2874 | 1.2905 | 1.1959 | 1.1604 |
| A3 | 0.9413 | 0.9411 | 0.8993 | 0.8547 | 0.8254 | 0.5302 | 0.7363 | 0.7217 |
| A4 | 0.9057 | 0.9087 | 0.8455 | 0.7987 | 0.6759 | 0.5137 | 0.5839 | 0.5794 |
| R2 | 0.9924 | 0.9847 | 0. 9678 | 0.9354 | 0.3718 | 0.3776 | 0.3515 | 0.3353 |
| R3 | 0.9818 | 0.9914 | 0.9853 | 0.9835 | 0.3588 | 0.3642 | 0.3403 | 0.3271 |
| D1 | 0.9707 | 0.9588 | 0.9307 | 0.8929 | 0.4045 | 0.4117 | 0.3952 | 0.3678 |
| D2 | 0.9349 | 0.9435 | 0.9862 | 0.9940 | 0.3882 | 0.2545 | 0.3832 | 0.3677 |
| D3 | 0.9339 | 0.9398 | 0.9739 | 0.9906 | 0.3609 | 0.3665 | 0.3520 | 0.3466 |
| D4 | 0.9969 | 0.9919 | 0.9914 | 0.9825 | 0.1259 | 0.1259 | 0.1239 | 0.1207 |
| F0 | 0.9461 | 0.9243 | 0.8601 | 0.7796 | 0.3993 | 0.4125 | 0.3695 | 0.3493 |
| F1 | 0.9036 | 0.9078 | 0.9252 | 0.9386 | 5.0485 | 5.0356 | 4.9084 | 4.8123 |
| F2 | 0.8368 | 0.8368 | 0.8368 | 0.8368 | 377963.4000 | 377963.4444 | 377962.7000 | 377961.4000 |
| F3 | 0.8368 | 0.8367 | 0.8368 | 0.8368 | 1.8898E+11 | 1.8898E+11 | 1.8898E+11 | 1.8898E+11 |

### 4.4. Calculation of the Kinetic parameters

According to the selected kinetic model D4, kinetic parameters are calculated in two steps; First, the curves of each temperature 23,29,35 and 45ºC are being drawn and then the value of kT is obtained by slope of the curve. Thus, four values for k are obtained. Second, according to Arrhenius integral equation, the slope of the obtained straight line from lnk versus 1/T shows the Ea, and the y-intercept shows the lnA. The data containing of Ea and 1/T of D4 model for releasing oxygen is shown in table 10. The value of Ea is equal to 12 as shown in table9.

**Table 10.** The kinetic parameters (Ea, K) of nanocomposite

| Kinetic parameters | 45 ºC | 35 ºC | 29 ºC | 23ºC |
|---|---|---|---|---|
| K | 0.0046 | 0.0052 | 0.0057 | 0.0065 |
| Ea(kJ/mol) | 12 | | | |
| $R^2$ | 0.9928 | | | |

### 5.3. characterization

The fiberglass matrix, as a moisture absorbent, can improve moisture absorption and increase the reaction rate, consequently. Also, since the plate structures have a higher surface to volume ratio (compared to tablet samples), due to the availability of more $KO_2$, the reaction rate is increased and the process of absorbing moisture and carbon dioxide, followed by the generation of oxygen at a faster rate. On the other hand, the synthesized nanocomposites under the EHD medium have uniform nanoparticles distributed on the fiberglass matrix (Fig. 7). Particles in the nanometer dimension have a higher reaction rate than larger particles, a fact that is seen in this reaction (the reaction rate of plates coated with superoxide nanoparticles is twice that of commercial samples).

Changing the particle size to nanometer dimensions, due to increasing the surface-to-volume ratio in the compounds, leads to an increase in the amount of effective substance available and speeds up the adsorption and conversion reactions. The presence of such a regular and uniform structure in this composition, leads to an increase in surface area, as the most available surface, causes the reaction to occur much faster, and then the reaction rate increases dramatically.

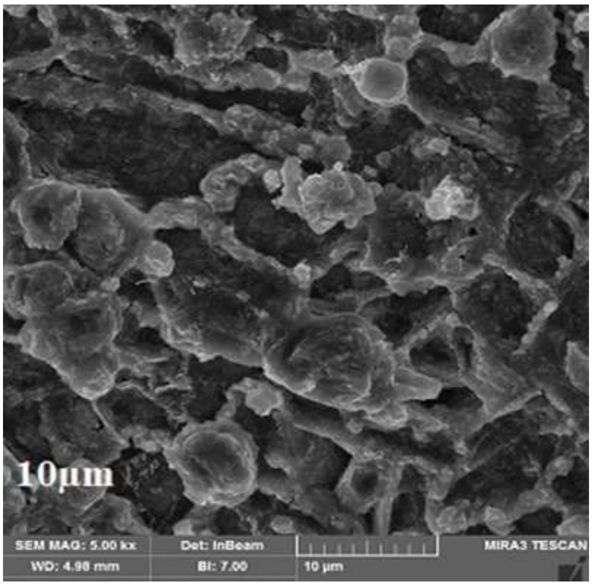


**Fig. 7.** FESEM image of $KO_2$-fiberglass nanocomposite synthesized by EHD method

### 4. Conclusion

In this study, potassium superoxide-fiberglass nanocomposite was synthesized by electrohydrodynamic (EHD) as an eco-technique. The results showed that the nanocomposite can be employed as an air revitalization component because increases and decreases $O_2$ and $CO_2$ amounts up to 29.4(%) and to half in 60min (twice faster than of commercial $KO_2$ samples), respectively. Besides, the increasing rate of $CO_2$ abortion and $O_2$ generation was performed by a higher amount of humidity (85%) and temperature (45ºC). With the air humidity increased (17% to 85%) the $CO_2$ absorption rate of nanocomposite increase about 1.5 times and $O_2$ generation increase about 1.3 times. Synthesis of potassium superoxide/fiberglass nanocomposite in EHD medium results in the formation of potassium superoxide nanoparticles uniformly on the fiberglass substrate and functionality of nanocomposite was improved by fiberglass support, because of its porosity which increased the adsorption ability of the final product. . Based on the results of statistical analysis on the modeling of reaction for oxygen releasing were shown that the best model for reaction is diffusion with equation of D4.

### Acknowledgments

We are grateful to the Malek Ashtar University of Technology for its financial support.

### References

[1] N. F. Gladyshev, T. V Gladysheva, S. I. Dvoretskii, S. B. Putin, M. A. Ul'yanova, and A. Ferapontov Yu, *Moscow, Mashinostroenie-1 Publ*, **2** (2007) 12.

[2] Y. A. Ferapontov, M. A. Ul'yanova, and T. V Sazhneva, *Russ. J. Appl. Chem.* **82 (**2009) 826.

[3] N. F. Gladyshev *et al.*, *Russ. J. Gen. Chem.* **84 (**2014) 2353.

[4] Y. Li and Y. Liu, *Int. J. Occup. Environ. Health*, **20 (**2014) 207.

[5] S. Wang, T. Zhang, and L. Jin, *Indoor Built Environ.* **28 (**2019) 599.

[6] N. Gao, H. Hu, X. Huang, L. Zhou, L. Fan, J. Min. Sci. Technol. **25** (2015) 151.

[7] L.-Z. Jin, S. Wang, S.-C. Liu, and Z. Zhang, *Combust. Sci. Technol.* **187** (2015) 1229

[8] M. A. Machado, D. A. Rodriguez, Y. Aly, M. Schoenitz, E. L. Dreizin, and E. Shafirovich, *Combust. Flame,* **161** (2014) 2708.

[9] E. Shafirovich, C. Zhou, S. Ekambaram, A. Varma, G. Kshirsagar, and J. E. Ellison, *Ind. Eng. Chem. Res.* **46** (2007) 3073.

[10] J. O. Stull and M. G. White, *Toxicol. Environ. Chem.* **10** (1985) 133.

[11] J. O. Stull, M. G. White, *Toxicol. Environ. Chem.* **10** (1985) 133.

[12] J. Li, L. Z. Jin, S. Wang, Z. Zhang, Y. Xu, and Q. K. Li, *Advanced Materials Research* **726** (2013) 363.

[13] A. W. Petrocelli, *Superoxides of the Alkali and Alkaline Earth Metals,* 1st ed., Springer (1966) pp. 91.

[14] S. V Mishchenko, P. V Balabanov, and A. A. Krimshtein, *Theor. Found. Chem. Eng.* **48** (2014) 306.

[15] A. Khawam, D.R. Flanagan, J. Phys. Chem. B, **109** (2005) 10073

[16] E. I. Trushliakov, "Indoor air comfort for human life support in living compartments of manned submersibles," SAE Technical Paper, 2006.

[17] M. Bamsey *Adv. Sp. Res.* **44** (2009) 151.

[18] J. H. Kim, Y. Park, and S. K. Jeong, *Korean J. Chem. Eng.* **27** (2010) 320

[19] S. G. Hosseini, M. Fathollahi, S. H. Motamedalshariaty, and R. Shokouhian, *J. Electrostat.* **108** (2020) 103522.

[20] Y. Zheng, M. Thiruvengadam, H. Lan, and C. J. Tien, *Int. J. Min. Sci. Technol.* **25** (2015) 927.

[21] K. J. Laidler, *J. Chem. Educ.* **61** (1984) 6.

[22] M. Fathollahi and H. Behnejad, *J of Applied Chemistry* **10** (1394) 85, in Persian

[23] J. Šesták and G. Berggren, *Thermochim. Acta* **3** (1979) 1.

[24] W. Hesse, M. Jansen, and W. Schnick, *Prog. solid state Chem.* **19** (1989) 47.

[25] I. I. Vol'nov and A. W. Petrocelli, *Peroxides, superoxides, and ozonides of alkali and alkaline earth metals*. Springer (1966) pp. 25

[26] K. R. Ward, G. S. Huvard, M. McHugh, R. R. Mallepally, and R. Imbruce, *Respir. Care*. **58** (2013) 184.

[27] S. Hui and C. Lin, *Environ. Sci. Manag.* **31** (2006) 79.